Molecular Cancer Research

Exploitation of Castration-Resistant Prostate Cancer Transcription Factor Dependencies by the Novel BET Inhibitor ABBV-075

Emily J. Faivre, Denise Wilcox, Xiaoyu Lin, Paul Hessler, Maricel Torrent, Wei He, Tamar Uziel, Daniel H. Albert, Keith McDaniel, Warren Kati, and Yu Shen

Abstract

Competitive inhibitors of acetyl-lysine binding to the bromodomains of the BET (bromodomain and extra terminal) family are being developed for the treatment of solid and hematologic malignancies. The function of BET family member BRD4 at enhancers/superenhancers has been shown to sustain signal-dependent or pathogenic gene expression programs. Here, the hypothesis was tested that the transcription factor drivers of castration-resistant prostate cancer (CRPC) clinical progression, including the androgen receptor (AR), are critically dependent on BRD4 and thus represent a sensitive solid tumor indication for the BET inhibitor ABBV-075. DHT-stimulated transcription of AR target genes was inhibited by ABBV-075 without significant effect on AR protein expression. Furthermore, ABBV-075 disrupted DHT-stimulated recruitment of BET family member BRD4 to gene-regulatory regions cooccupied by AR, including the well-established PSA and TMPRSS2 enhancers. Persistent BET inhibition disrupted the composition and function of AR-occupied enhancers as measured by a reduction in AR and H3K27Ac ChIP signal and inhibition of enhancer RNA transcription. ABBV-075 displayed potent antiproliferative activity in multiple models of resistance to second-generation antiandrogens and inhibited the activity of the AR splice variant AR-V7 and ligand-binding domain gain-of-function mutations, F877L and L702H. ABBV-075 was also a potent inhibitor of *MYC* and the TMPRSS2-ETS fusion protein, important parallel transcription factor drivers of CRPC.

Implications: The ability of BET family inhibitor ABBV-075 to inhibit transcription activation downstream of the initiating events of transcription factors like AR and TMPRSS2:ETS fusion proteins provides a promising therapeutic option for CRPC patients who have developed resistance to second-generation antiandrogens. *Mol Cancer Res; 15(1); 35–44. ©2016 AACR.*

Introduction

Bromodomains are conserved protein folds that recognize and bind acetylated lysines. The four members of the BET family (bromodomain and extra-terminal, BRD2, BRD3, BRD4, and BRDt) exhibit a high degree of homology across their two N-terminal bromodomains (1). BET proteins localize to chromatin via bromodomain interaction with acetylated lysines on the tails of histones and subsequently recruit pTEFb and large complexes, such as Mediator to coordinate multiple aspects of transcription (2). In addition to these more general effects on transcription, the bromodomains of BET proteins can bind to acetyl-lysines on transcription factors, including NF-κB and TWIST to specify gene expression in a signal-dependent manner (3, 4). Furthermore, a disproportionate amount of BRD4 in a cell is reported to localize to large enhancers/superenhancers to "turbo-charge" stemness or pathogenic gene expression programs (5, 6). These observations suggest that BET proteins function as signal-dependent specificity factors to coordinate the output of critical gene expression programs.

Competitive inhibitors of the BET bromodomain interaction with acetyl-lysine displace BET proteins from chromatin to affect changes (primarily inhibition) in transcription; in doing so, BET inhibitors are largely broadly active anticancer agents. In light of the specific role performed by BRD4 in the regulation of signal-induced transcription and output of large enhancers, we hypothesized that select tumor types with an established dependence on aberrant transcription factors would display particular sensitivity to the antiproliferative effects of the potent orally bioavailable novel BET inhibitor, ABBV-075 (7). Herein, we have focused on prostate cancer as a representative transcription-dependent tumor type where the majority of disease incidence and progression is driven by the androgen receptor (AR), a ligand-activated nuclear receptor superfamily member.

During normal development, the AR regulates genes that are important for the differentiation of the prostate gland. However, in prostate cancer, AR transcription factor function is redirected to drive the malignant phenotype. Consistent with this observation, patients with locally advanced or metastatic disease will initially respond to first-line androgen deprivation therapy. Unfortunately, nearly all will recur with lethal locally advanced or metastatic castration-resistant prostate cancer (mCRPC). At this point in disease progression, men with advanced or metastatic CRPC receive second-generation hormone therapies that block either

AbbVie Inc., North Chicago, Illinois.

Note: Supplementary data for this article are available at Molecular Cancer Research Online (http://mcr.aacrjournals.org/).

Corresponding Authors: Emily J. Faivre, AbbVie Inc., 1 North Waukegan Rd., North Chicago, IL 60064. Phone: 847-938-5456; Fax: 847-935-0014; E-mail: emily.faivre@abbvie.com; and Yu Shen, Phone: 847-936-1128; Fax: 847-935-0014; E-mail: yu.shen@abbvie.com

doi: 10.1158/1541-7786.MCR-16-0221

androgen production (abiraterone) or function as direct AR antagonists (enzalutamide). These agents significantly prolong survival in men with metastatic CRPC, but inevitably, resistance emerges and the patients will succumb to their disease. Again, reassertion of the AR pathway is evident, supported by reports of AR ligand-binding domain (LBD) mutations or splice variants that lack the LBD (8–12). In addition to AR, transcription factors, such as the ETS family, a frequent translocation target in prostate cancer, or MYC overexpression may operate in concert with or parallel to AR to promote invasion or resistance to hormonal therapy. Unfortunately, to date, these transcription programs have not previously been amenable to pharmacologic targeting. Together, continual reactivation of the AR pathway, the outlier expression of ETS proteins, and MYC overexpression underscore the importance of transcription factors to drive the malignant state of prostate cancer.

Using prostate cancer and its dependence on AR as a model system, we investigated the role of BRD4 in signal-dependent transcription and the therapeutic potential of BET inhibitors in a transcription-driven indication. We report a functional interaction between BRD4 and AR that is required for androgen-activated epigenetic alterations and transcription of AR target genes that translates into *in vivo* tumor growth inhibition. Together, these data indicate a mechanism-based antitumor activity profile for the BET inhibitor ABBV-075 in preclinical models of hormone therapy–resistant CRPC and support clinical development of ABBV-075 for the treatment of recurrent mCRPC.

Materials and Methods

Cell lines and compounds

All cell lines were originally obtained from ATCC and subsequently maintained by a Core Cell Line Facility that performed routine testing for mycoplasma and authentication by short tandem repeat (STR) analysis using the Gene Print10 Kit (Promega). LNCaP-FGC, MDV_R, 22RV-1, PC-3, and DU145 were grown in RPMI1640 + 10% FBS (Gibco), and VCaP were grown in DMEM + 10%FBS (Gibco). MDA-PCa-2b were grown in HPC-1 media + 20% FBS on plates coated with FNC Coating Mix (AthenaES). ABBV-075 was synthesized by AbbVie, enzalutamide was purchased from Selleck Chemicals, and ARN-509 was purchased from ChemScene.

Generation of acquired resistance to enzalutamide

LNCaP-FGC cells were continuously grown in the presence of 1 μmol/L enzalutamide for >3 months until the outgrowth of resistant cells appeared. The pooled population was named MDV_R, STR confirmed to be derived from LNCaP-FGC cells, and the resistance phenotype was stably maintained in the absence of enzalutamide for >4 weeks.

Gene expression

RNA was harvested using the Pure Link Kit (Life Technologies); cDNA was made with the High-Capacity cDNA Reverse Transcription (RT) Kit (Applied Biosystems). qPCR was performed with TaqMan Universal Master Mix and Probes (Life Technologies), and analyzed using the $\Delta\Delta C_t$ method. For microarray studies, RNA was prepared by Qiazol extraction followed by RNeasy mini column (QIAGEN) and target preparation was executed using 3′ IVT Plus Amplification Kit (Affymetrix). Subsequently, samples were hybridized to Human Genome U133 Plus 2.0 chip and scanned with the Affymetrix scanner. Analysis, including fold change and cluster analysis, was performed with Rosetta Resolver Gene Expression Data Analysis System Version 7.2 and subjected to pathway analysis [Ingenuity Pathway Analysis (IPA), Qiagen]. The gene expression array data can be found at the Gene Expression Omnibus under accession number GSE86245.

Western blot analysis

Cell lysates were prepared in RIPA Buffer (Thermo Scientific) supplemented with protease inhibitor cocktail tablets (Roche), and total protein was measured by Bradford method. Equal amount of protein was resolved in 3% to 8% Tris-Acetate Gels (NuPage, Life Technologies), transferred to nitrocellulose using the iBlot system (Invitrogen), and probed with primary antibodies specific for AR, PSA (CST), β-actin (Sigma) or BRD2, BRD3, or BRD4 (Bethyl Laboratories). Signal was visualized using a Li-Cor instrument subsequent to 1-hour incubation with appropriate IR-conjugated secondary antibodies.

Cell viability, cell cycle, and senescence

For viability assays, CellTiter-Glo Reagent (Promega) was added directly to media, and luminescence was measured using an Enspire luminometer (PerkinElmer). To measure cell-cycle distribution, cells were fixed with 70% ethanol (EtOH), followed by incubation with the Guava Cell Cycle Reagent and analysis using the Guava easyCyte (Millipore). Senescence was measured using the reagents and protocol from the β-galactosidase Kit (CST).

Chromatin immunoprecipitation qPCR

Confluent LNCaP-FGC cells were treated as described, then fixed for 10 minutes with direct addition of 1% formaldehyde (Thermo Scientific). The fixation was stopped with 1.25 mmol/L glycine (Sigma) for 5 minutes, followed by wash and collection in cold PBS and subsequent lysis [1% SDS, 10 μmol/L EDTA, 50 μmol/L Tris-Cl pH 8.0, 5 mmol/L sodium butyrate (Sigma), protease inhibitor cocktail tables (Roche)]. Chromatin was sheared to 300 to 500 kb using the Bioruptor (Diagenode). Lysates were mixed 1:4 with Dilution Buffer (0.01% SDS, 1.1% Triton X-100, 1.2 μmol/L EDTA, 16.7 μmol/L Tris-Cl pH 8.0, 167 μmol/L NaCl, 5 mmol/L sodium butyrate, protease inhibitor cocktail tablet). Immunoprecipitation was performed by the IP-Star (Diagenode) with anti-AR (Millipore), -BRD4 (Bethyl) -H3K27Ac (Active Motif), or -GATA2 (EpiGentek) antibodies and Protein A or G Dynabeads (Life Technologies). Chromatin immunoprecipitates were washed once with TE and three times with Wash Buffer (100 mmol/L Tris-Cl pH 8.0, 500 mmol/L LiCl, 15 Igepal, 1% deoxycholic acid) supplemented with PMSF. Beads were resuspended in Elution Buffer (20 mmol/L $NaHCO_3$, 1% SDS, 150 mmol/L NaCl), and cross-links were reversed overnight at 65°C, followed by 1-hour RNase A and proteinase K digestion at 45°C. DNA was purified using chromatin immunoprecipitation (ChIP) DNA Clean & Concentrator (Zymo). qPCR was performed with SYBR (Perfecta, Quanta), using specific primers to *KLK3*/PSA promoter (5′-CCTAGATGAAGTCTCCATGAGCTACA, 5′-GGGAGGGAGAGCTAGCACTTG), *KLK3*/PSA enhancer (5′-TGGGACAACTTGCAAACCTG, 5′-CCAGAGTAGGTCTGTTTTCAATCCA), *TMPRSS2* ARE V (5′-TGGTCCTGGATGATAAAAAAAGTTT, 5′-GACATACGCCCCACAACAGA), *MYC* EpiTect ChIP qPCR Assay NM_002467.3 (-)01Kb), and analyzed using $\Delta\Delta C_t$ method with

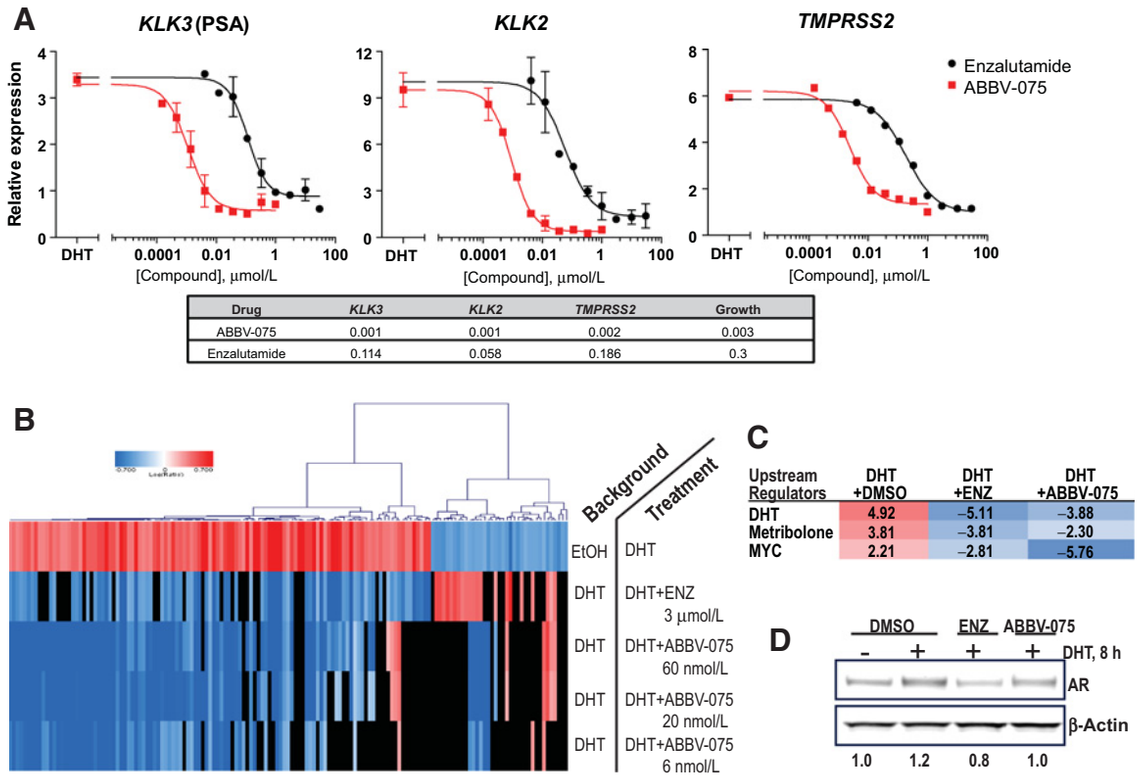

Figure 1.

ABBV-075 inhibits the AR gene expression pathway in hormone-sensitive prostate cancer. **A,** qRT-PCR dose response of ABBV-075 versus enzalutamide in the presence of 5 nmol/L DHT for 6 hours in LNCaP-FGC cells. Inhibitors were added 45 minutes prior to DHT addition. Each data point represents the average from biological replicates from two independent experiments. Bottom, correlation between target gene EC_{50}s and 5-day growth inhibition (μmol/L). **B,** Gene expression profiling cluster diagram showing dose-dependent ABBV-075 inhibition of DHT-stimulated genes. **C,** IPA upstream regulator analysis of microarray data indicated potent activation of hormone pathways (DHT, and metribolone, aka R1881) and MYC transcriptional networks following DHT stimulation with highly significant Z-scores. ABBV-075 and enzalutamide reversed the pathway activation as shown by the negative Z-scores. **D,** Representative Western blot analysis ($n = 3$) showing ABBV-075 (50 nmol/L) does not affect AR protein levels. Densitometry for AR signal (normalized to β-actin) indicated below.

negative control regions *GAD1* (Abcam Ab85780) or *MYOD* (Abcam Ab85776).

Murine prostate tumor xenograft model

All animal studies were conducted in a specific pathogen-free environment in accordance with the Internal Institutional Animal Care and Use Committee (IACUC, accredited by the American Association of Laboratory Animal Care under conditions that meet or exceed the standards set by the United States Department of Agriculture Animal Welfare Act, Public Health Service policy on humane care and use of animals, and the NIH guide on laboratory animal welfare, IACUC protocol ID 1503D00007). For tumor engraftment, a 1:1 mixture of LNCAP-FGC cells (ATCC) and Matrigel (BD Biosciences) was inoculated (5×10^6 cells/site) subcutaneously into the right hind flank of male NSG mice (The Jackson Laboratory). Daily administration of compound or vehicle was initiated at the time of size match randomization 15 days postinoculation ($n = 9$ per group) and continued for 4 weeks. The tumors were measured by a pair of calipers twice a week, and tumor volumes were calculated according to the formula $V = L \times W^2/2$ (V: volume, mm^3; L: length, mm; W: width, mm). Tumor growth inhibition, %TGI = 100 − mean tumor volume of treatment group/mean tumor volume of control group × 100. The Tukey–Kramer HSD (honest significant difference) test was used to compare mean tumor volumes.

Results

ABBV-075 inhibits ligand-activated AR transcription factor function

To evaluate the requirement for BET proteins in AR-dependent signaling, we performed qRT-PCR to measure AR target gene transcription in androgen (DHT)-stimulated LNCaP-FGC prostate cancer cells. The transcript levels of *KLK3* (PSA), *KLK2*, and *TMPRSS2* increased 3- to 9-fold over the vehicle control (EtOH) following 6 hours of DHT stimulation (Fig. 1A). As expected, the direct AR antagonist enzalutamide blocked DHT activation of target gene transcription in a dose-dependent manner. The BET inhibitor ABBV-075 also inhibited DHT activation of *KLK3*, *KLK2*, and *TMPRSS2* transcription in a dose-dependent manner. AR target genes were likewise reduced by ABBV-075 in the AR-dependent cell lines VCaP and MDA-PCa-2b (Fig. 5A and C). In support of a specific role for BET proteins in AR transcription factor function, ABBV-075 potently inhibited transcription from an

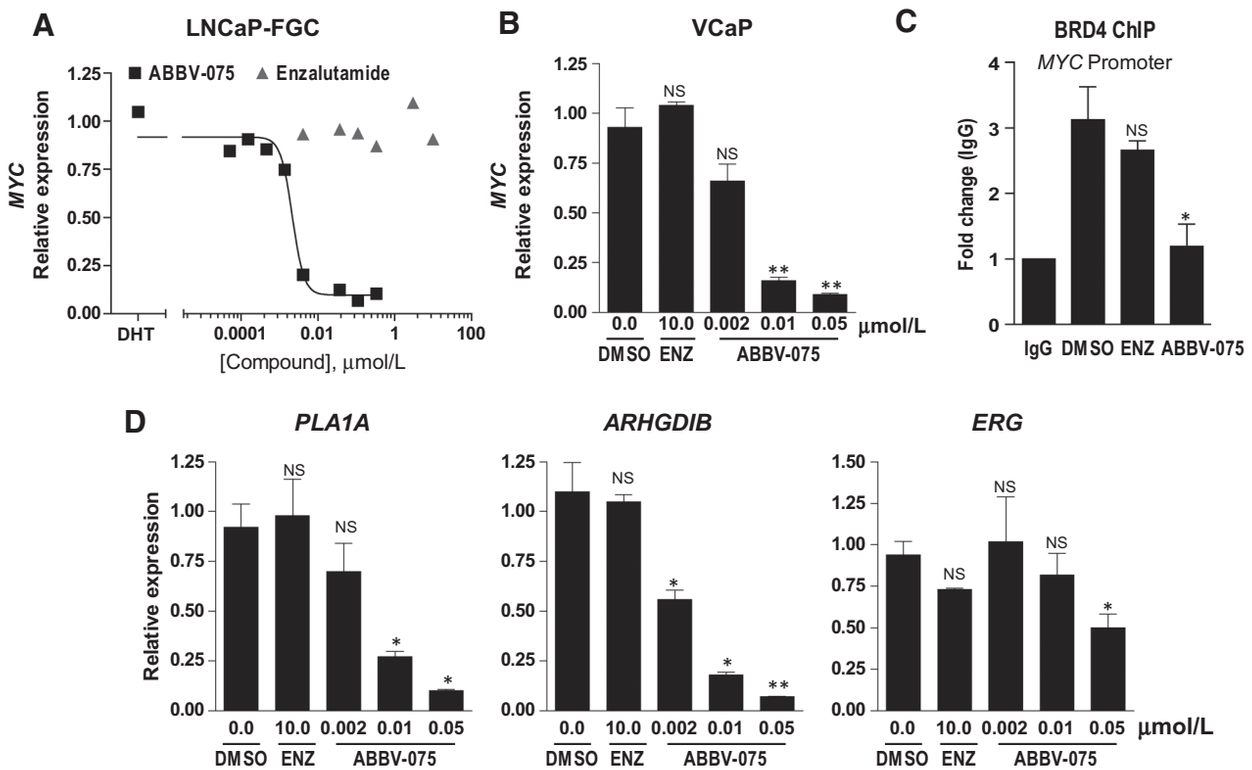

Figure 2.

ABBV-075 inhibits *MYC* and ETS target gene transcription. **A,** qRT-PCR dose-dependent reduction of *MYC* transcripts by ABBV-075 but not enzalutamide in LNCaP-FGC cells treated with DHT for 6 hours. **B,** Reduction of *MYC* transcripts by ABBV-075 but not enzalutamide in VCaP cells treated for 24 hours. **C,** ChIP qPCR measurement of BRD4 displacement from *MYC* by ABBV-075 (50 nmol/L) but not enzalutamide in LNCaP-FGC cells. **D,** Twenty-four–hour treatment with ABBV-075 but not enzalutamide inhibits *PLA1A and ARHGDIB* expression in TMPRSS2:ERG fusion positive VCaP cells, measured by qRT-PCR. All data shown are representative of two to three independent experiments. Bars, mean of duplicates + SD. Statistical significance compared with vehicle control was determined by two-tailed Student *t* tests: *, $P < 0.05$; **, $P < 0.01$; NS, not significant.

ARE-luciferase reporter construct (Supplementary Fig. S1A). Strikingly, the IC_{50}s for ABBV-075 and enzalutamide inhibition of AR in functional assays (qRT-PCR and ARE-luc) closely approximates the antiproliferative EC_{50}s in normal and DHT-stimulated growth conditions (Fig. 1A, bottom and Supplementary Fig. S1B). The correlation between inhibition of AR function and prostate cancer cell growth by both enzalutamide and ABBV-075 suggests that AR requires BET proteins to fully enact its role as the primary driver of prostate cancer cell line growth.

To interrogate the scope of BET protein regulation of AR output, we performed RNA profiling experiments. DHT stimulation of LNCaP-FGC cells incurred significant changes in gene expression (>2 fold, $P < 0.01$) in both the up- (115 genes) and down (38 genes) direction over the EtOH vehicle control (Fig. 1B). IPA analysis revealed a significant enrichment of DHT-induced gene expression changes that fall within the DHT signature (Fig. 1C). Genes that were stimulated by DHT were specifically blocked both by enzalutamide and by ABBV-075 in a dose-dependent manner, with deep penetrance of inhibition by ABBV-075 into the DHT gene list (Fig. 1B). Enzalutamide, but not ABBV-075, blocked DHT-induced downregulation of target genes, indicating a role for BET proteins in AR transcription activation but not inhibition. ABBV-075 inhibition of DHT-stimulated AR target gene activation occurred without significant effect on AR protein (Fig. 1D). Thus, ABBV-075 blocks the requisite contribution of BET proteins to the ligand-stimulated activation of AR target genes.

Inhibition of *MYC* and ETS pathway by ABBV-075

As shown in Fig. 1C, IPA analysis indicated that the MYC pathway was significantly upregulated in response to DHT and blocked both by enzalutamide and ABBV-075. We therefore investigated whether *MYC* was a direct transcription target of AR and BET proteins in prostate cancer. *MYC* transcripts did not change dramatically in response to DHT stimulation of LNCaP-FGC cells and were not affected by enzalutamide (Fig. 2A and B). In contrast, ABBV-075 dramatically inhibited *MYC* in LNCaP-FGC cells (Fig. 2A) and in the VCaP cell line, respectively (Fig. 2B). This result is consistent with the displacement of BRD4 from *MYC*-regulatory regions by ABBV-075 but not by enzalutamide (Fig. 2C). In prostate cancer, MYC expression has been reported to be regulated by the transcription factor ERG and contributes to CRPC progression (13, 14). The *ERG* gene and related ETS family member *ETV1* are frequent translocation targets in prostate cancer and associated overexpression augments invasion and metastasis (15, 16). We investigated the BET family dependence of the ETS pathway transcription factor function in three translocation models, VCaP (*TMPRSS2:ERG*), LNCaP, and MDA-PCa-2b

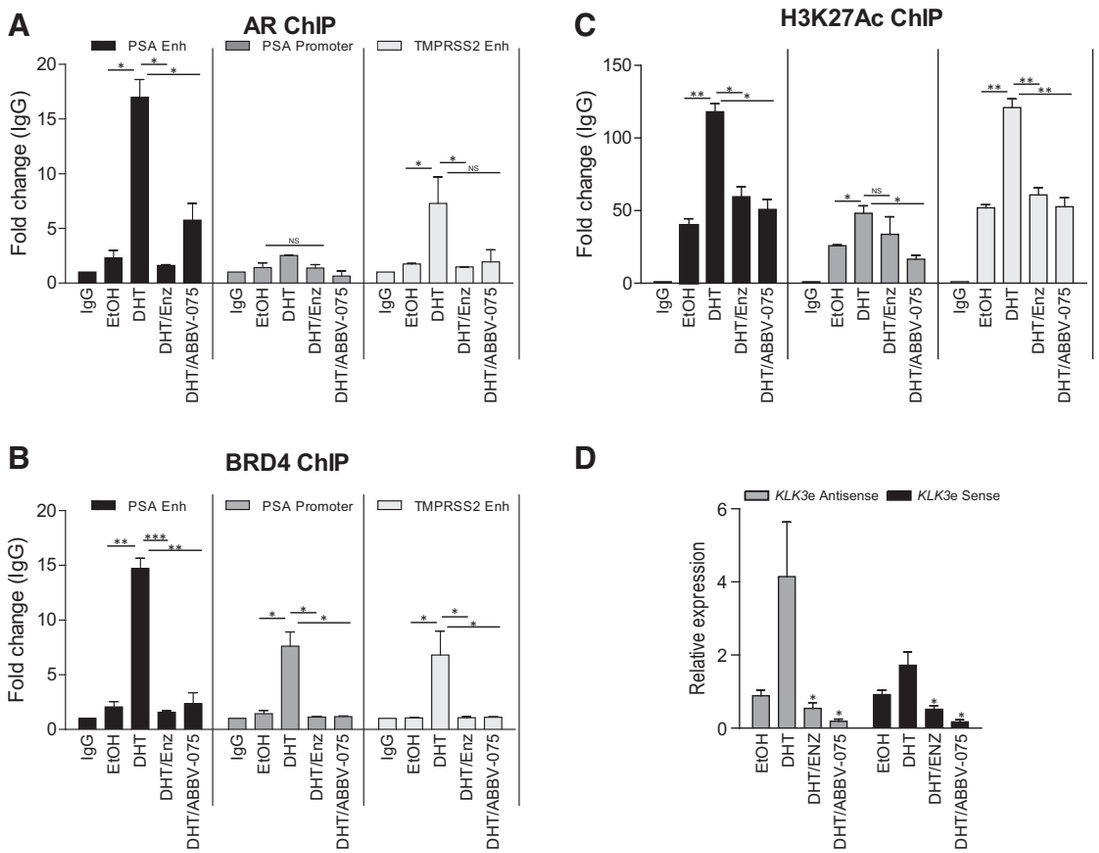

Figure 3.

DHT stimulates BRD4 recruitment and remodeling of AR-occupied enhancer. **A,** ChIP-qPCR in LNCaP-FGC cells demonstrating AR occupancy of the PSA enhancer (ARE III) and promoter and *TMPRSS2* enhancer (ARE V) is stimulated by DHT (5 nmol/L, 24 hours) and inhibited by enzalutamide (3 μmol/L) and ABBV-075 (60 nmol/L) pretreatment (45 minutes). **B,** DHT-stimulated BRD4 localization to *TMPRSS2* and PSA enhancers is blocked by enzalutamide and ABBV-075. **C,** DHT (5 nmol/L, 6 hours) increased H3K27Ac signal in ChIP-qPCR at ARE enhancers in an AR and BET- bromodomain-dependent manner, as shown by reduced enrichment in the presence of enzalutamide (3 μmol/L) or ABBV-075 (50 nmol/L). **A–C,** bars indicate the mean + SD of two to three independent biological replicates. **D,** qRT-PCR measurement of DHT-increased transcription in the forward (sense) and reverse (antisense) direction from the *KLK3* enhancer was inhibited by ABBV-075 and enzalutamide. Bars indicate mean + SD of duplicates and are representative of three independent experiments. Statistical significance compared with vehicle control was determined by two-tailed Student *t* tests: *, $P < 0.05$; **, $P < 0.01$; ***, $P < 0.005$; NS, not significant.

(14q13-14q21.1 *ETV1* translocation; ref. 15). ABBV-075 significantly reduced the expression of ETS family target genes *ARHGDIB* and *PLA1A* in VCaP (Fig. 2D), LNCaP, and MDA-PCa-2b cells (Supplementary Fig. S2). Direct reduction of *ERG* and *ETV1* transcripts at the highest concentration of ABBV-075 (50 nmol/L; Fig. 1D and Supplementary Fig. S2) may contribute in part to the inhibition of ETS target genes, including *MYC*.

BRD4 is recruited to AR-occupied chromatin in a DHT-dependent manner

We next conducted ChIP qPCR studies to probe the signal-dependent contribution of BET proteins to AR activation. As shown in Fig. 3A, DHT stimulation of LNCaP-FGC cells induced a robust recruitment of AR to the *KLK3* (PSA) and *TMPRSS2* enhancers compared with control (EtOH). Minimal AR was measured at the PSA promoter. DHT-stimulated AR recruitment was blocked by enzalutamide. Under control conditions, BRD4 was not detected significantly above background levels, indicating the BRD4 is not substantially preloaded at ARE enhancer sites (Fig. 3B). DHT stimulation triggered a robust recruitment of BRD4 to all three regulatory regions measured: ABBV-075 pretreatment completely blocked DHT-stimulated BRD4 redistribution (Fig. 3B). DHT-stimulated BRD4 occupancy at the *KLK3* (PSA) and *TMPRSS2* enhancers was also blocked by enzalutamide, suggesting that the DHT-stimulated recruitment of BRD4 to ARE enhancers requires AR and is AR ligand binding dependent. To test this idea, inhibitors were added subsequent to DHT-stimulated recruitment of AR. Enzalutamide addition following 3 hours of DHT (post-) was unable to displace pre-bound AR from the *KLK3* (PSA) and *TMPRSS2* enhancers (Supplementary Fig. S3A). Posttreatment with enzalutamide also failed to displace BRD4 (Supplementary Fig. S3B); thus, the persistence of AR correlated with retention of BRD4. In contrast, addition of ABBV-075 in the posttreatment condition fully displaced BRD4 similar to pretreatment (Supplementary Fig. S3B).

As shown in Fig. 3A, we also noted that ABBV-075 affected the degree of AR recruitment to the PSA and *TMPRSS2* enhancers,

Table 1. IC_{50} values (μmol/L) for enzalutamide and ABBV-075 in 5-day growth assay in multiple cell line models of enzalutamide resistance

IC_{50}, (μmol/L)	LNCaP-FGC	MDV_R	MDA-PCa-2b	22RV1	VCaP	PC-3	DU-145
AR status	T878A	T878A, F877L	T878A, L702H	AR-V7	Amp, AR-V7	Neg	Neg
Enzalutamide	0.55	>30	>30	>30	>30	>30	>30
ABBV-075	0.003	0.001	0.007	0.006	0.011	0.112	0.238

NOTE: AR status is indicated for each cell line.

consistent with the previously reported effects of JQ1, a validated BET inhibitor tool compound, on global AR chromatin binding in VCaP cells (17, 18). ABBV-075 neither reduced the expression of AR pioneer factors FOXA1 or GATA2 (Supplementary Fig. S3C) nor disrupted GATA2 occupancy at the ARE enhancers (data not shown). To explore whether ABBV-075's effect on AR chromatin binding related to BRD4's function as a multivalent scaffold protein that both engages and stabilizes large enhancers, we performed ChIP for the active enhancer mark H3K27Ac. H3K27Ac was readily detected at the PSA enhancer and promoter and the *TMPRSS2* enhancer in unstimulated cells (Fig. 3C). Interestingly, DHT significantly augmented H3K27Ac levels at both the PSA and *TMPRSS2* enhancers, while more modest changes were measured at the PSA promoter. ABBV-075 and enzalutamide blocked the DHT-stimulated increase in H3K27Ac at ARE enhancers but had no effect on basal levels. Transcription of noncoding enhancer RNA (eRNA), including at the PSA enhancer, performs a regulatory function for the activation of neighboring genes (19), and BRD4 has been reported to stimulate eRNA synthesis through bromodomain interactions with acetylated histones (20). We therefore measured DHT-stimulated transcription from the PSA enhancer in both the forward and reverse directions as a corollary for BRD4's role in nascent ARE enhancer function. Increased *KLK3* eRNA transcription following DHT stimulation was blocked by both enzalutamide and ABBV-075 (Fig. 3D), providing additional evidence that AR and BRD4 are both required to orchestrate ARE enhancer composition and function.

Antitumor activity of ABBV-075

In light of the signal-dependent functional interaction between BRD4 and AR, and the correlation between target gene inhibition and antiproliferative IC_{50}s for ABBV-075 and enzalutamide, we pursued additional phenotypic evidence that BRD4 and AR function in the same pathway. First, the antiproliferative profiles of enzalutamide and ABBV-075 were similarly associated with AR expression, as neither agent incurred potent growth inhibition in the AR negative prostate cancer cell lines PC-3 and DU145 (Table 1). Second, treatment with both agents sustained significant G_1 arrest with concomitant S-phase depletion (Fig. 4A). ABBV-075 induced potent G_1 arrest in a dose-dependent manner (Supplementary Fig. S4A). Prolonged exposure to ABBV-075 and enzalutamide led to a senescent phenotype as shown by the β-galactosidase–associated staining (Fig. 4B and Supplementary Fig. S4B), a purported contributor to the efficacy of other G_1 arrest agents, such as palbociclib (21). ABBV-075 has excellent drug-like properties and is being studied in a phase I clinical trial (trial registration ID: NCT02391480); therefore, we evaluated the *in vivo* antitumor activity of ABBV-075 in LNCaP-FGC flank xenograft experiments. Tumor-bearing mice were dosed once daily with ABBV-075 (1 mg/kg/day) or enzalutamide (20 mg/kg/day) for 4 weeks. ABBV-075 and enzalutamide induced comparable tumor growth inhibition (Fig. 4C) in the hormone-dependent prostate cancer model.

Antiproliferative activity of ABBV-075 across multiple models of resistance to second-generation antiandrogens

The lack of durable responses to second-generation hormone therapies in CRPC patients is postulated to result from a reassertion of the AR pathway (22). Our results suggest that BRD4 functions at a critical node downstream of AR-ligand binding (Figs. 1 and 3); therefore, we investigated the conservation of ABBV-075 antitumor activity in the face of acquired or intrinsic resistance to enzalutamide. As shown in Table 1, among the five tested AR-positive prostate cancer cell lines, enzalutamide inhibited the growth of only the hormone-dependent LNCaP-FGC cell line, proving an ineffective antiproliferative agent in VCaP, MDA-PCa-2b, 22RV1, or MDV_R cell lines. Each cell line in the panel represents a unique mechanism of resistance to enzalutamide (detailed below). Strikingly, ABBV-075 maintained antiproliferative activity in all models, consistent with our data that AR transcription activation requires BRD4 as a cofactor downstream of ligand binding.

ABBV-075 is active against AR-amplified and AR-variant models of enzalutamide resistance

Expression of AR splice variants that lack the C-terminal LBD has emerged as a potential resistance mechanism to enzalutamide. Both the VCaP and 22RV1 cell lines express the AR-V7 splice variant and are resistant to enzalutamide's antiproliferative activity (Supplementary Fig. S5A; Table 1). To determine whether ABBV-075 could inhibit AR-V7 activity in the setting of enzalutamide resistance, we treated VCaP cells with enzalutamide or three doses of ABBV-075 and measured the effect on transcript levels of *KLK3* (PSA) and an AR-V7 target gene, *UBE2C* (23). ABBV-075 potently inhibited the transcription of *KLK3* and *UBE2C*, with partial or no effect of a high dose of enzalutamide, respectively (Fig. 5A). In addition to AR-V7 expression, VCaP cells harbor *AR* amplification, which may explain the reduced sensitivity of *KLK3* levels to enzalutamide. Similar to Chan and colleagues (18), we detected a modest but significant reduction in AR-V7–specific transcripts and protein with ABBV-075 treatment (Fig. 5A and Supplementary Fig. S5C), which may in part account for the reduction in *UBE2C* transcripts. Finally, ABBV-075 but not enzalutamide induced a robust senescent response in the setting of AR-V7 resistance to enzalutamide (Fig. 5B and Supplementary Fig. S5E).

ABBV-075 is active against AR LBD mutation models of enzalutamide resistance

The MDA-PCa-2b cell line was likewise sensitive to ABBV-075 antiproliferative activity in 5-day growth and protracted senescence studies but resistant to enzalutamide (Table 1; Fig. 5B and Supplementary Fig. S5B). An AR-positive cell line from a patient who failed androgen ablation therapy (Supplementary Fig. S5A; ref. 24), *KLK2* transcripts were significantly reduced following 6 and 24 hours treatment with ABBV-075, but only minor response was measured with enzalutamide (Fig. 5C). Notably, the AR LBD

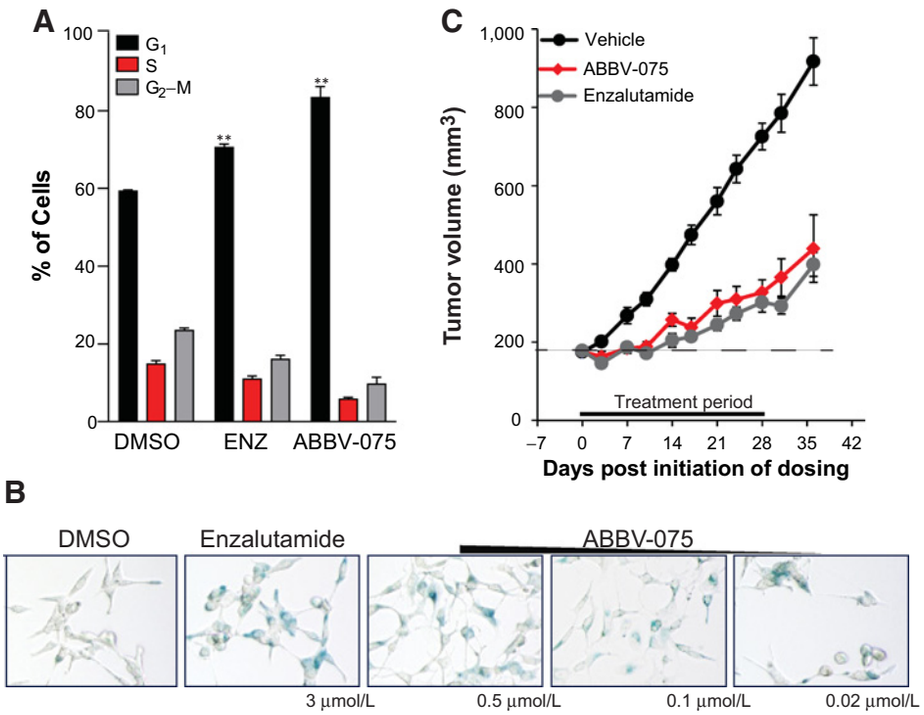

Figure 4.

Enzalutamide and ABBV-075 exhibit comparable antitumor phenotypes. **A,** ABBV-075 caused G_1 arrest in LNCaP-FGC cells as indicated by percent distribution in G_1, S, or G_2–M after 72 hours of treatment with 500 nmol/L ABBV-075, 3 µmol/L enzalutamide, or DMSO control. Statistical significance for G_1 distribution compared with vehicle control was determined by two-tailed Student *t* tests: **, $P < 0.01$. **B,** Twelve-day treatment with enzalutamide and ABBV-075 induced senescence in LNCaP-FGC cells as measured by blue β-galactosidase staining. **C,** Comparable tumor growth inhibition (TGI, %) between ABBV-075 and enzalutamide in the hormone-sensitive LNCaP-FGC xenograft model. Study was conducted as a flank tumor model in male NSG mice, $n = 8$ for each group, once daily dosing for 28 days. Significant weight loss (cachexia) was measured across all dosing cohorts (vehicle, 22%; ABBV-075: 22%; enzalutamide, 17%). Mean tumor volume for the ABBV-075 and the enzalutamide groups differed significantly ($P < 0.05$) from vehicle group starting on day 10. No significant differences were observed between the two treatment groups throughout the study.

in this cell line contains two mutations: T878A also found in LNCaP-FGC AR that confers activation by corticosteroids; and L702H in Helix 3 that has been reported in approximately 5% of clinical samples (25). The L702H mutation is insensitive to bicalutamide antagonism (26), consistent with the apparent intrinsic resistance to enzalutamide's antagonism of AR and antiproliferative activity observed in our studies. Indeed, an in-house molecular modeling study (Schrödinger Release 2015-1: Maestro, version 10.1, Schrödinger, LLC, 2015; PyMOL Molecular Graphics System, Version 1.4 Schrödinger, LLC) reveals that the Helix 3 L702 residue points toward the Helix 10 F877 residue acting as a putative LBD gatekeeper, blocking/enabling access to Helix-12, and also controlling the size of the LBD (Supplementary Fig. S5B). The larger mutant histidine residue harbored by the MDA-PCa-2b AR at position 702 may restrict the access of enzalutamide to the AR LBD but remains susceptible to ABBV-075 inhibition of the AR pathway.

To test the activity of ABBV-075 in a model of acquired resistance to enzalutamide, we performed routine culture of LNCaP-FGC cells in the presence of enzalutamide until the outgrowth of a resistant population (Supplementary Fig. S6A). Growth assays with this cell line, named MDV_R, revealed a greater than 100-fold resistance to enzalutamide (Table 1) and cross-resistance to ARN-509 (Supplementary Fig. S6B), a third-generation antiandrogen in clinical development. At the molecular level, MDV_R cells were AR positive (Supplementary Fig. S6C), and enzalutamide displayed agonistic activity, increasing *KLK2* and *KLK3* transcripts similar to DHT alone (Fig. 5D and Supplementary Fig. S6E). Sequencing revealed a single missense mutation resulting in the amino acid change of phenylalanine at position 877 to leucine (F877L; Supplementary Fig. S6D). The F877L mutation was previously reported as a gain-of-function mutation that conferred enzalutamide resistance and was detected in patients with biochemical progression while receiving ARN-509 and enzalutamide (8, 9, 11, 12). In contrast to the enzalutamide's agonism of F877L AR activity in the MDV_R cells, ABBV-075 treatment significantly downregulated *KLK2* and *KLK3* transcripts without a strong effect on AR itself (Fig. 5D and Supplementary Fig. S6E). ABBV-075 also maintained potent antiproliferative activity (Table 1) and induced a senescent phenotype (Fig. 5B and Supplementary Fig. S5E) in MDV_R cells expressing the gain-of-function F877L AR.

Discussion

Herein, we provide the first report of a clinical-grade BET family inhibitor in models of AR-dependent prostate cancer and detail the mechanism of action for ABBV-075 antitumor

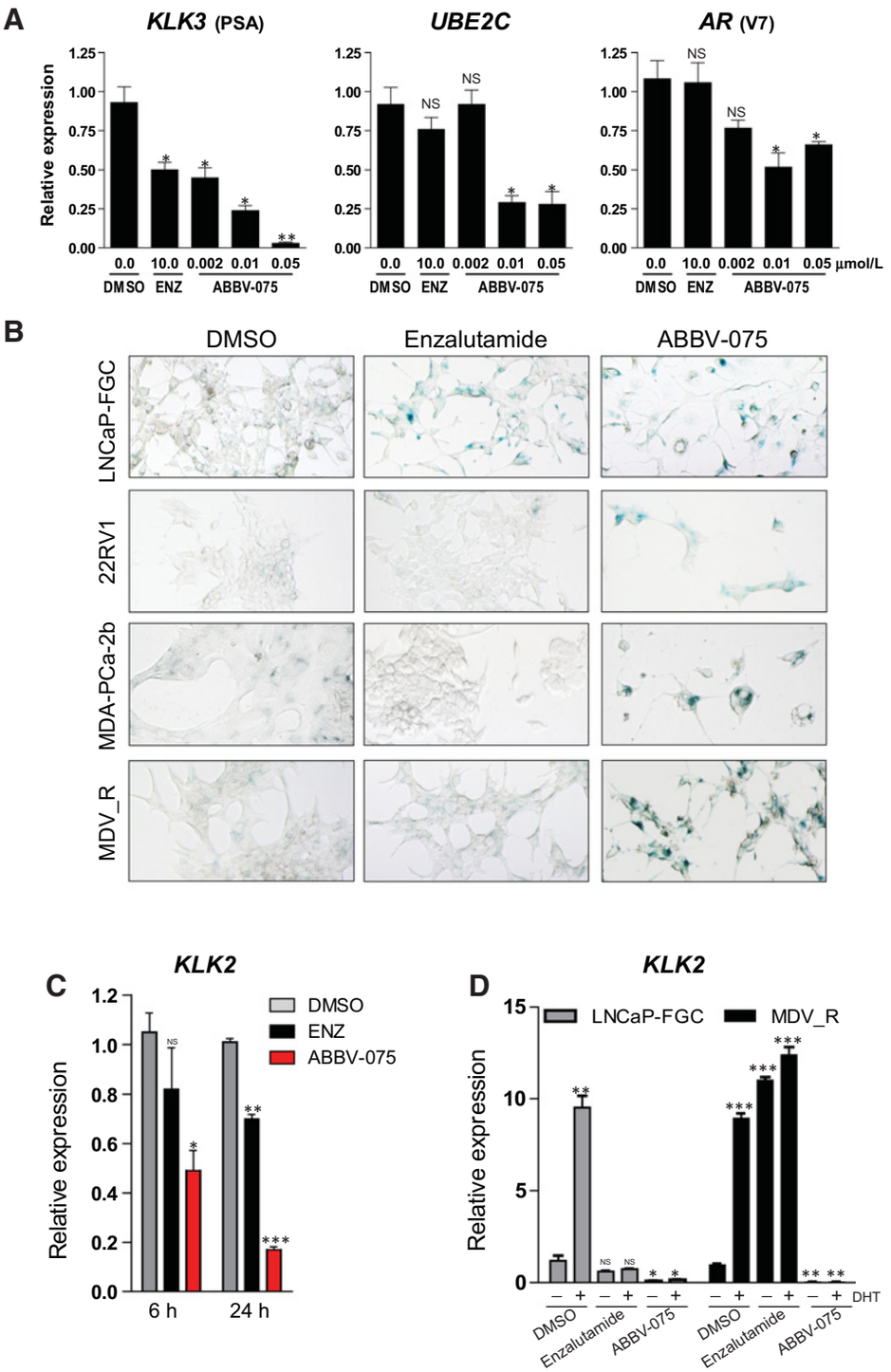

Figure 5.
ABBV-075 activity in AR-V7 and AR-LBD mutation models of enzalutamide resistance. **A,** ABBV-075 effectively inhibits expression of *KLK3* (PSA) and the AR-V7 target gene *UBE2C* in VCaP cells that are *AR* amplified, AR-V7 positive. In contrast, enzalutamide has reduced antagonism of *KLK3* and no effect on *UBE2C* expression. **B,** ABBV-075 induced senescence in 22RV1, MDA-PCa-2b, and MDV_R cell line models of enzalutamide resistance. **C,** ABBV-075 inhibited the AR target gene *KLK2* in MDA-PCa-2b cells that have intrinsic enzalutamide resistance. **D,** qRT-PCR results demonstrating that ABBV-075, acting downstream of AR ligand binding, potently inhibited DHT-stimulated *KLK2* expression in MDV_R cells with a gain-of-function AR mutation (F877L) that confers agonism of AR by enzalutamide. Statistical significance compared with vehicle control was determined by two-tailed Student *t* tests: *, $P < 0.05$; **, $P < 0.01$; ***, $P < 0.005$; NS, not significant.

activity. We show that BRD4 functionally interacts with AR at well-defined ARE-containing enhancers in a DHT-dependent manner. Enhancer colocalization of BRD4 with AR occurs subsequent to AR ligand binding. The accumulation of BRD4 at AR-occupied enhancers is concomitant with an increase in the active histone mark H3K27Ac and eRNA transcription. This signal-dependent BRD4-mediated epigenome remodeling is likely a key component of the persistent activation of the AR gene signature. We also show that ABBV-075 disrupts enhancer assembly in response to DHT stimulation by displacing both BRD4 and AR from the chromatin, reducing the deposition of H3K27Ac, and inhibiting eRNA transcription. In turn, ABBV-075 potently blocked DHT-stimulated transcription of AR target genes. Consequently, ABBV-075 inhibited the growth of

AR-dependent prostate cancer cell lines, inducing G_1 arrest and ultimately causing a senescent phenotype. ABBV-075 performed comparably with enzalutamide in androgen-dependent *in vivo* xenograft studies, demonstrating potent tumor growth inhibition. Consistent with a BET-dependent mechanism of action downstream of androgen binding, we show that ABBV-075 maintains inhibition of the AR pathway and potent antiproliferative activity in AR-V7 and LBD mutation models of enzalutamide resistance. Finally, we also show that ABBV-075 inhibits *MYC* and the ETS pathways, two well-recognized transcription factors that contribute to CRPC progression by augmenting metastasis or hormone therapy resistance but are not currently tractable. ABBV-075's action against multiple transcription dependencies of prostate cancer demarcates the therapeutic advantage of development of a BET inhibitor for CRPC patients that have failed their second-generation hormone therapies.

The development of BET inhibitors has been an active area of research both in academia and industry, with numerous clinical trials in phase I/II, sponsored by more than 10 different companies. BET inhibitors are broadly antiproliferative across multiple *in vitro* cell line models; however, the leading indication for clinical development has been hematologic malignancies, such as AML and multiple myeloma. This may in part be due to elicitation of an apoptotic response by BET inhibitors, including ABBV-075 (Bui and colleagues, submitted; ref. 27). For solid tumor indications, the challenge has been to identify tumor types with intrinsic sensitivity to BET inhibitors to effectively increase therapeutic indices. Herein, we endeavored to capitalize on the reported dependence of oncogenic transcription programs on BET proteins to drive the output from large enhancers/superenhancers. To this end, we found that the robust antiproliferative activity of ABBV-075 correlated with inhibition of the AR pathway in prostate cancer and furthermore exploits the persistent reactivation of the AR pathway in multiple models of enzalutamide resistance. Consistent with previous reports using the tool BET inhibitor compound JQ1 (17), we likewise measured a significant reduction in the expression of ETS target genes by treatment with ABBV-075 in three separate models of ETS gene rearrangements. Downregulation of ETS expression combined with the reported disruption of BRD4 interaction with acetylated ETS transcription factors (28, 29) implies two hits on the TMPRSS2:ETS pathway. Although the majority of our data strongly indicate ABBV-075 inhibits AR function independent of an effect on AR expression, it is noteworthy that VCaP AR-FL (full length) protein and transcripts were modestly reduced by the highest dose of ABBV-075 (Supplementary Fig. S5C and S5D). Therefore, although low concentrations of ABBV-075 (<0.01 μmol/L) clearly inhibit AR function independent of AR transcripts in LNCaP and VCaP cells (Fig. 5A), it is possible that reduction of AR-FL may contribute to pathway inhibition at higher ABBV-075 concentrations similar to the two hits on TMPRSS2:ETS. Collectively, our results and evidence from the literature support a model whereby the capacity of BET proteins to "turbo-charge" transcription is coopted to meet the demands of transcription-addicted cancer cells and suggest that other transcription factor–dependent indications, such as ER^+ breast cancer (30), will likewise prove sensitive to ABBV-075.

The clinical success of second-generation antiandrogens has been transformative for mCRPC patients; however, nearly all will relapse and succumb to their disease. Multiple mechanisms are likely to drive the resistance phenotype, but the emergence of AR LBD mutations and splicing variants lacking the LBD reiterate the paradigm of addiction to the AR for disease progression (22). Although rational design of novel therapeutics to address each individual mutation has been proposed (9), our data support a model whereby inhibition of AR downstream of activation with ABBV-075 may offer a more comprehensive approach to targeting the multiple resistance states. In summary, we have outlined a mechanism for BET inhibitor sensitivity in AR-dependent prostate cancer, wherein the AR pathway functionally interacts with BRD4 at enhancers to reorganize the local chromatin composition and drive an oncogenic transcription program. Similar dependence on BET proteins by parallel pathways that contribute to CRPC progression, such as the ETS pathway and *MYC*, expand on the potential therapeutic benefit that ABBV-075 could deliver in the setting of recurrent mCRPC.

Disclosure of Potential Conflicts of Interest

All authors are employees of AbbVie. The design, study conduct, and financial support for this research were provided by AbbVie. AbbVie participated in the interpretation of data, review, and approval of the publication. No other potential conflicts of interest were disclosed.

Authors' Contributions

Conception and design: E.J. Faivre, D. Wilcox, D.H. Albert, Y. Shen
Development of methodology: E.J. Faivre, D. Wilcox, X. Lin, D.H. Albert
Acquisition of data (provided animals, acquired and managed patients, provided facilities, etc.): E.J. Faivre, D. Wilcox, X. Lin, P. Hessler, W. He, T. Uziel, D.H. Albert
Analysis and interpretation of data (e.g., statistical analysis, biostatistics, computational analysis): E.J. Faivre, D. Wilcox, X. Lin, P. Hessler, M. Torrent, T. Uziel, D.H. Albert, Y. Shen
Writing, review, and/or revision of the manuscript: E.J. Faivre, W. He, D.H. Albert, K. McDaniel, W. Kati, Y. Shen
Administrative, technical, or material support (i.e., reporting or organizing data, constructing databases): E.J. Faivre
Study supervision: E.J. Faivre, K. McDaniel, Y. Shen
Other (development of chemical tools utilized in the study): K. McDaniel

The costs of publication of this article were defrayed in part by the payment of page charges. This article must therefore be hereby marked *advertisement* in accordance with 18 U.S.C. Section 1734 solely to indicate this fact.

Received July 1, 2016; revised September 15, 2016; accepted September 22, 2016; published OnlineFirst October 5, 2016.

References

1. Filippakopoulos P, Picaud S, Mangos M, Keates T, Lambert JP, Barsyte-Lovejoy D, et al. Histone recognition and large-scale structural analysis of the human bromodomain family. Cell 2012;149:214–31.
2. Wu SY, Chiang CM. The double bromodomain-containing chromatin adaptor Brd4 and transcriptional regulation. J Biol Chem 2007;282:13141–5.
3. Brown JD, Lin CY, Duan Q, Griffin G, Federation AJ, Paranal RM, et al. NF-kappaB directs dynamic super enhancer formation in inflammation and atherogenesis. Mol Cell 2014;56:219–31.
4. Shi J, Wang Y, Zeng L, Wu Y, Deng J, Zhang Q, et al. Disrupting the interaction of BRD4 with diacetylated Twist suppresses tumorigenesis in basal-like breast cancer. Cancer Cell 2014;25:210–25.

5. Loven J, Hoke HA, Lin CY, Lau A, Orlando DA, Vakoc CR, et al. Selective inhibition of tumor oncogenes by disruption of super-enhancers. Cell 2013;153:320–34.
6. Whyte WA, Orlando DA, Hnisz D, Abraham BJ, Lin CY, Kagey MH, et al. Master transcription factors and mediator establish super-enhancers at key cell identity genes. Cell 2013;153:307–19.
7. Wang L, Pratt JK, McDaniel KF, Dai Y, Fidanze SD, Hasvold L, et al. , inventors. AbbVie, Inc., assignee. Bromodomain inhibitors. United States patent US20140162971 A1. 2014 Jun 12.
8. Joseph JD, Lu N, Qian J, Sensintaffar J, Shao G, Brigham D, et al. A clinically relevant androgen receptor mutation confers resistance to second-generation antiandrogens enzalutamide and ARN-509. Cancer Discov 2013;3:1020–9.
9. Balbas MD, Evans MJ, Hosfield DJ, Wongvipat J, Arora VK, Watson PA, et al. Overcoming mutation-based resistance to antiandrogens with rational drug design. Elife 2013;2:e00499.
10. Antonarakis ES, Lu C, Wang H, Luber B, Nakazawa M, Roeser JC, et al. AR-V7 and resistance to enzalutamide and abiraterone in prostate cancer. N Engl J Med 2014;371:1028–38.
11. Azad AA, Volik SV, Wyatt AW, Haegert A, Le Bihan S, Bell RH, et al. Androgen receptor gene aberrations in circulating cell-free DNA: biomarkers of therapeutic resistance in castration-resistant prostate cancer. Clin Cancer Res 2015;21:2315–24.
12. Korpal M, Korn JM, Gao X, Rakiec DP, Ruddy DA, Doshi S, et al. An F876L mutation in androgen receptor confers genetic and phenotypic resistance to MDV3100 (enzalutamide). Cancer Discov 2013;3:1030–43.
13. Sun C, Dobi A, Mohamed A, Li H, Thangapazham RL, Furusato B, et al. TMPRSS2-ERG fusion, a common genomic alteration in prostate cancer activates C-MYC and abrogates prostate epithelial differentiation. Oncogene 2008;27:5348–53.
14. Cho H, Herzka T, Zheng W, Qi J, Wilkinson JE, Bradner JE, et al. RapidCaP, a novel GEM model for metastatic prostate cancer analysis and therapy, reveals myc as a driver of Pten-mutant metastasis. Cancer Discov 2014;4:318–33.
15. Tomlins SA, Laxman B, Dhanasekaran SM, Helgeson BE, Cao X, Morris DS, et al. Distinct classes of chromosomal rearrangements create oncogenic ETS gene fusions in prostate cancer. Nature 2007;448:595–9.
16. Tomlins SA, Laxman B, Varambally S, Cao X, Yu J, Helgeson BE, et al. Role of the TMPRSS2-ERG gene fusion in prostate cancer. Neoplasia 2008;10:177–88.
17. Asangani IA, Dommeti VL, Wang X, Malik R, Cieslik M, Yang R, et al. Therapeutic targeting of BET bromodomain proteins in castration-resistant prostate cancer. Nature 2014;510:278–82.
18. Chan SC, Selth LA, Li Y, Nyquist MD, Miao L, Bradner JE, et al. Targeting chromatin binding regulation of constitutively active AR variants to overcome prostate cancer resistance to endocrine-based therapies. Nucleic Acids Res 2015;43:5880–97.
19. Hsieh CL, Fei T, Chen Y, Li T, Gao Y, Wang X, et al. Enhancer RNAs participate in androgen receptor-driven looping that selectively enhances gene activation. Proc Natl Acad Sci U S A 2014;111:7319–24.
20. Kanno T, Kanno Y, LeRoy G, Campos E, Sun HW, Brooks SR, et al. BRD4 assists elongation of both coding and enhancer RNAs by interacting with acetylated histones. Nat Struct Mol Biol 2014;21:1047–57.
21. Thangavel C, Dean JL, Ertel A, Knudsen KE, Aldaz CM, Witkiewicz AK, et al. Therapeutically activating RB: reestablishing cell cycle control in endocrine therapy-resistant breast cancer. Endocr Relat Cancer 2011;18:333–45.
22. Watson PA, Arora VK, Sawyers CL. Emerging mechanisms of resistance to androgen receptor inhibitors in prostate cancer. Nat Rev Cancer 2015;15:701–11.
23. Hu R, Lu C, Mostaghel EA, Yegnasubramanian S, Gurel M, Tannahill C, et al. Distinct transcriptional programs mediated by the ligand-dependent full-length androgen receptor and its splice variants in castration-resistant prostate cancer. Cancer Res 2012;72:3457–62.
24. Navone NM, Olive M, Ozen M, Davis R, Troncoso P, Tu SM, et al. Establishment of two human prostate cancer cell lines derived from a single bone metastasis. Clin Cancer Res 1997;3:2493–500.
25. Robinson D, Van Allen EM, Wu YM, Schultz N, Lonigro RJ, Mosquera JM, et al. Integrative clinical genomics of advanced prostate cancer. Cell 2015;161:1215–28.
26. Zhao XY, Boyle B, Krishnan AV, Navone NM, Peehl DM, Feldman D. Two mutations identified in the androgen receptor of the new human prostate cancer cell line MDA PCa 2a. J Urol 1999;162:2192–9.
27. Conery AR, Centore RC, Spillane KL, Follmer NE, Bommi-Reddy A, Hatton C, et al. Preclinical anticancer efficacy of BET bromodomain inhibitors is determined by the apoptotic response. Cancer Res 2016;76:1313–9.
28. Roe JS, Mercan F, Rivera K, Pappin DJ, Vakoc CR. BET bromodomain inhibition suppresses the function of hematopoietic transcription factors in acute myeloid leukemia. Mol Cell 2015;58:1028–39.
29. Blee AM, Liu S, Wang L, Huang H. BET bromodomain-mediated interaction between ERG and BRD4 promotes prostate cancer cell invasion. Oncotarget 2016 May 20. [Epub ahead of print].
30. Feng Q, Zhang Z, Shea MJ, Creighton CJ, Coarfa C, Hilsenbeck SG, et al. An epigenomic approach to therapy for tamoxifen-resistant breast cancer. Cell Res 2014;24:809–19.